New biostratigraphic, magnetostratigraphic and isotopic insights into the Middle Eocene Climatic Optimum in low latitudes

Edgar, K. M.; Wilson, P. A.; Sexton, P. F.; Gibbs, S. J.; Roberts, A. P.; Norris, R. D.

DOI:
10.1016/j.palaeo.2010.09.016

Document Version
Peer reviewed version

Citation for published version (Harvard):
Edgar, KM, Wilson, PA, Sexton, PF, Gibbs, SJ, Roberts, AP & Norris, RD 2010, 'New biostratigraphic, magnetostratigraphic and isotopic insights into the Middle Eocene Climatic Optimum in low latitudes', *Palaeogeography Palaeoclimatology Palaeoecology*, vol. 297, no. 3-4, pp. 670-682. https://doi.org/10.1016/j.palaeo.2010.09.016

New biostratigraphic, magnetostratigraphic and isotopic insights into the Middle Eocene Climatic Optimum in low latitudes

K.M. Edgar[a]*, P.A. Wilson[a], P.F. Sexton[a, b, c], S.J. Gibbs[a], A.P. Roberts[a, d] and R.D. Norris[b]

[a] School of Ocean and Earth Science, National Oceanography Centre, Southampton, SO14 3ZH, UK.

[b] Scripps Institution of Oceanography, University of California, San Diego, La Jolla, CA 92093, USA.

[c] now at: School of Earth and Ocean Sciences, Cardiff University, Cardiff CF10 3YE, UK.

[d] now at: Research School of Earth Science, The Australian National University, Canberra ACT 0200, Australia.

*Corresponding author. Tel.: +44-2380-596245; Fax; +44-2380-593052

E-mail address: kme@noc.soton.ac.uk

Abstract

The Middle Eocene Climatic Optimum (MECO) was a warming event that interrupted the long-term Eocene cooling trend. While this event is well documented at high southern and mid-latitudes, it is poorly known from low latitudes and its timing and duration are not well constrained because of problems of hiati, microfossil preservation and weak magnetic polarity in key sedimentary sections. Here, we report the results of a study designed to improve the bio-, magneto- and chemostratigraphy

of the MECO interval using high-resolution records from two low-latitude sections in the Atlantic Ocean, Ocean Drilling Program (ODP) Sites 1051 and 1260. We present the first detailed benthic foraminiferal stable isotope records of the MECO from the low latitudes as well as biostratigraphic counts of *Orbulinoides beckmanni* and new magnetostratigraphc results. Our data demonstrate a ~750 kyr-long duration for the MECO characterized by increasing $\delta^{13}C$ and decreasing $\delta^{18}O$, with minimum $\delta^{18}O$ values lasting ~40 kyrs at 40.1 Ma coincident with a short-lived negative $\delta^{13}C$ excursion. Thereafter, $\delta^{18}O$ and $\delta^{13}C$ values recover rapidly. The shift to minimum $\delta^{18}O$ values at 40.1 Ma is coincident with a marked increase in the abundance of the planktonic foraminifera *O. beckmanni*, consistent with its inferred warm-water preference. *O. beckmanni* is an important Eocene biostratigraphic marker, defining planktonic foraminiferal Zone E12 with its lowest and highest occurrences (LO and HOs). Our new records reveal that the LO of *O. beckmanni* is distinctly diachronous, appearing ~500 kyr earlier in the equatorial Atlantic than in the subtropics (40.5 versus 41.0 Ma). We also show that, at both sites, the HO of *O. beckmanni* at 39.5 Ma is younger than published calibrations, increasing the duration of Zone E12 by at least 400 kyr. In accordance with the tropical origins of *O. beckmanni*, this range expansion to higher latitudes may have occurred in response to sea surface warming during the MECO and subsequently disappeared with cooling of surface waters.

Keywords: Middle Eocene Climatic Optimum, Site 1051, Site 1260, planktonic foraminifera, biostratigraphy, magnetostratigraphy.

1. Introduction

Development of high-quality age models is essential for the reliable determination of

sequences of events in the geological record, i.e., a geological timescale, for correlation of palaeorecords between sites, and for estimating rates of change in palaeoenvironmental records. Construction of a reliable geological time scale for the middle Eocene has been hindered by a lack of high quality sedimentary sections. In part, these difficulties arise from a relatively shallow calcite compensation depth (CCD) in the Eocene compared to the modern day, which has resulted in comparatively poor preservation of contemporaneous carbonate microfossils in deep-sea sediments, particularly in the Pacific Ocean (Lyle et al., 2005). Weak palaeomagnetic signals typical of carbonate-rich Palaeogene sediments are a further complication for the calibration of biostratigraphic datums. Therefore, typically, deep-sea sections with good microfossil preservation are characterized by poor magnetostratigraphies (e.g., Ocean Drilling Program, ODP Legs 143, 154, 198 and 208; Sager et al., 1993; Curry et al., 1995; Bralower et al., 2002; Zachos et al., 2004;), while those with good magnetostratigraphies suffer poor calcareous microfossil preservation (e.g., ODP Leg 199; Lyle et al., 2002). Similarly, in the classic land-based exposures in Italy (e.g., Gubbio) that constitute the magnetostratigraphic reference for a large part of the Eocene, calcareous microfossils are also typically poorly preserved and the magnetostratigraphy can be ambiguous (Lowrie et al., 1982; Napoleone et al., 1983; Jovane et al., 2007; Luciani et al., 2010).

One interval of Eocene time for which it has proven particularly problematic to obtain high quality sections (because of recovery difficulties), is the chron C18r/18n boundary and planktonic foraminiferal Zone E12 (Berggren and Pearson, 2005), the interval in which the MECO falls (Bohaty et al., 2009) (Fig. 1). Biozone E12 is defined by the total range of the short-lived tropical planktonic foraminiferal species

Orbulinoides beckmanni. *O. beckmanni* is a particularly useful biostratigraphic marker because, first, it divides what would otherwise be a long (~4 Myr) biozone, stretching from the highest occurrence (HO) of *Guembelitriodes nuttalli* at 42.3 Ma to the HO of *Morozovelloides crassatus* at 38.0 Ma, Zones E11-E13 (Berggren and Pearson, 2005) (Fig. 1). Second, the existing calibration for Zone E12 is coincident with the MECO (Fig. 1) (Sexton et al., 2006a; Bohaty et al., 2009), which raises the possibility that *O. beckmanni* might represent an 'excursion' taxon akin to those documented for the Paleocene-Eocene Thermal Maximum (Kelly et al., 1996, 1998). However, the relatively poor recovery of Zone E12 by deep-sea drilling has hindered direct calibration of this Zone to the geomagnetic polarity time-scale (GPTS). A near global hiatus near the chron C18r/C18n boundary at ~40.0 Ma truncates the top of planktonic foraminiferal Zone E12 in many deep-sea sequences (e.g., Karig et al., 1975; Erbacher et al., 2004), while other sequences are limited by the presence of chert or condensation horizons (Zachos et al., 2004), a lack of carbonate (Lyle et al., 2002), poor magnetostratigraphic control or the absence of the marker species *O. beckmanni* (e.g., Sager et al., 1993; Curry et al., 1995; Bralower et al., 2002; Zachos et al., 2004).

Here we present new high-resolution magnetic polarity data from Site 1051 alongside quantitative records of the biostratigraphic marker species *O. beckmanni* and benthic foraminiferal stable isotope records from ODP Site 1051 and, for comparison, similar records from Site 1260 in the Atlantic Ocean. ODP Site 1051 represents an ideal section to address the above stratigraphic issues because, on the basis of available records, it has a high sedimentation rate for a deep-sea site in the middle Eocene (~4 cm/kyr), it is stratigraphically continuous (at least to biozone and magnetochron

level), it hosts sediments that are suited to develop a resolvable magnetostratigraphy and it is situated well above the local CCD, favouring preservation of calcareous microfossils (Shipboard Scientific Party, 1998). For comparison, ODP Site 1260 also benefits from a good magnetostratigraphy and carbonate microfossil preservation, but the sedimentary succession is truncated by a hiatus at the chron C18r/18n boundary (Shipboard Scientific Party, 2004; Suganuma and Ogg, 2006). These new datasets are used to: (1) improve the magnetostratigraphic resolution of the late middle Eocene interval at Site 1051, (2) refine the existing biomagnetostratigraphic calibrations at Sites 1051 and 1260, (3) assess the chronological reliability of the bioevents that define Zone E12 at Sites 1051 and 1260, (4) test whether the MECO is present in these tropical and northern hemisphere sites and (5) determine if the speciation or subsequent extinction of *O. beckmanni* are linked to the MECO.

2. Locations and geological setting

ODP Site 1051 (30°03'N; 76°21'W, modern water depth 1980 meters below sea level, mbsl) is situated on the Blake Nose plateau in the western North Atlantic Ocean (Fig. 2). The estimated palaeodepth for Site 1051 is 1000 - 2000 mbsl for the middle Eocene (Shipboard Scientific Party, 1998) with a palaeolatitude of ~25ºN (Ogg and Bardot, 2001). Site 1051 comprises a stratigraphically complete (at least to magnetochron level) expanded late Paleocene through middle Eocene sequence of siliceous nannofossil oozes interspersed with approximately 25 thin ash horizons (Shipboard Scientific Party, 1998). Estimated sedimentation rates are ~ 1 to 4 cm/kyr.

ODP Site 1260 (9°16'N; 54°33'W, modern water depth 2549 mbsl) (Fig. 2) was drilled on the Demerara Rise plateau (palaeowater depths for the Eocene close to

126 those of the present day, Arthur and Natland, 1979) and was situated at a
127 palaeolatitude of 1ºS in the middle Eocene (Suganuma and Ogg, 2006). Middle
128 Eocene sediments at Site 1260 are primarily greenish grey nannofossil chalks with
129 foraminifers and radiolarians (Shipboard Scientific Party, 2004), with average
130 sedimentation rates across the focal interval of ~2 cm/kyr.
131
132 **3. Methods**
133 ***3.1 Palaeomagnetism***
134 To generate a continuous high-resolution magnetic polarity record across Zone E12
135 at Site 1051, u-channel samples were taken following the shipboard composite depth
136 section splice (Shipboard Scientific Party, 1998) between 66.15 and 146.63 meters
137 composite depth (mcd). Below ~150 mcd, sediments were recovered using the
138 extended core barrel, which makes them less suitable for detailed analysis.
139
140 All u-channel samples were measured on a 2-G Enterprises cryogenic magnetometer
141 (at the National Oceanography Centre, Southampton) after progressive stepwise
142 alternating field (AF) demagnetization at successive peak fields of 5, 10, 15, 20, 25,
143 30, 40, 50 and 60 milliTesla (mT), and occasionally up to 80 mT. The natural
144 remanant magnetization (NRM) was measured at 1 cm stratigraphic intervals,
145 although smoothing occurs because of the width of the magnetometer response
146 function (half-width = 5 cm). Thus, data from the top and bottom 5 cm of each u-
147 channel were excluded from this study because of edge effects (Roberts, 2006). The
148 inclination and declination of the characteristic remanant magnetization (ChRM) was
149 determined at 1 cm intervals using principal component analysis; with data from at
150 least 4 demagnetization steps, and the quality of the linear regressions was estimated

by calculating the maximum angular deviation associated with the best-fit line (Kirschvink, 1980). The age model for Site 1260 is based on Suganuma and Ogg (2006), which was supplemented by additional palaeomagnetic measurements by Edgar et al. (2007).

3.2 Orbulinoides beckmanni *abundance counts*

To determine the LO and HO of *Orbulinoides beckmanni*, high-resolution relative abundance counts (percent of total planktonic foraminifera) were produced for sample splits of ~400 individuals from 482 samples at 10 cm sampling resolution (mean sampling interval of 3 kyr) for ODP Site 1051 and on 69 samples at ~30 cm sampling resolution (sampling interval 12 kyr) at ODP Site 1260. Samples were prepared for abundance counts by washing 20 cm^3 of bulk sediment over a 63 μm mesh and then dry sieved at 300 μm. Biozonations and taxonomy adopted for this study are those of Berggren and Pearson (2005), and Proto-Decima and Bolli (1970) and Premoli Silva et al. (2006), respectively. We distinguish *O. beckmanni* from its immediate ancestor *Globigerinatheka euganea* (see Plates I and II) by the presence of spiral sutural apertures between early chambers (Plate IIb,f and h) and more numerous (>4) smaller, sutural apertures in the last few chambers, e.g., Plate II, specimens a,e, i, j and l. An additional diagnostic criterion is the presence of small, circular apertures within the wall of the last few large chambers (areal apertures; see Plate II, specimens a, c, i, j and l), commonly found in *O. beckmanni* but never reported in any of the globigerinathekids (Premoli-Silva et al., 2006). Thus, when present, areal apertures are a useful diagnostic characteristic.

3.3 Oxygen and carbon isotope measurements

Benthic foraminiferal stable isotope ($\delta^{18}O$ and $\delta^{13}C$) data were generated using the species *Cibicidoides eoceanus* (Site 1260) and *Oridorsalis umbonatus* (Site 1051), following taxonomy employed by Tjalsma and Lohmann (1983) and van Morkhoven et al. (1986). Foraminifera were picked from the size range 250-350 μm and were cleaned by ultrasonication prior to isotopic analysis. Benthic foraminifera are relatively sparse at Site 1051 owing to dilution by siliceous microfossils. At Site 1260 benthic foraminifera are more abundant and sufficient individuals for stable isotope analysis (~3-5) were found in every sample examined. All stable isotope measurements were determined using a Europa GEO 20-20 mass spectrometer equipped with an automatic carbonate preparation system (CAPS). Results are reported relative to the Vienna Pee Dee Belemnite (VPDB) standard with an external analytical precision of 0.07‰ and 0.03‰ for $\delta^{18}O$ and $\delta^{13}C$, respectively. Stable isotope values generated from *Cibicidoides eoceanus* are adjusted to equilibrium by adding 0.28‰ VPDB to $\delta^{18}O$ values, following the Palaeogene correction factor for *Cibicidoides* (Katz et al., 2003) and 0.72‰ VPDB is added to the $\delta^{13}C$ values of *Oridorsalis umbonatus* to normalise to *Cibicidoides* (Katz et al., 2003).

4. RESULTS

4.1 Palaeomagnetic behavior and polarity zonation

U-channel samples from Site 1051 have comparatively weak magnetizations (~10^{-5} to 10^{-4} Am^{-1}), typical of carbonate-rich sediments, but with stable and readily interpreted palaeomagnetic behavior (Fig. 3a-f). Samples are characterized by a small, low-stability steeply dipping normal polarity component (Fig. 3a-f) that is interpreted to be as a drilling overprint. This magnetic overprint was successfully removed with peak AFs of <20 mT. The ChRM of the u-channel samples in the more strongly

magnetized composite section (108 – 146 mcd; Fig. 4) was isolated between 20 and 50 mT and, toward the top of the composite section (~68 and 108 mcd), between the 5 and 25 mT demagnetization steps (because of the less stable demagnetization behavior in this upper interval, Fig. 3g and h). This is not ideal, and particular care was taken to discard data in this interval if there was a suggestion of an unremoved drilling overprint.

Magnetic polarity intervals were determined based on the clustering of positive or negative inclinations. Our new data from between 65 and 150 mcd provide a substantial improvement on the published lower-resolution dataset available between 0 and 150 mcd (Shipboard Scientific Party, 1998; Ogg and Bardot, 2001) (Fig. 4). Five distinct magnetozones (R1 to R3) are identified (Fig. 4), in our new dataset and the boundaries between these improved from a previous resolution of ±2.5 m (Ogg and Bardot, 2001) to between < 2 cm and ~ 1 m (Table 1).

Within each of the 'long' magnetozones investigated (N1 through N2) are a number of short-lived (~2-8 kyr) polarity intervals, e.g., at 128 and 130 mcd (Fig. 4). The majority of these short-lived polarity features are associated with large increases in the measured NRM intensity (Fig. 4) and are likely to reflect measurement artifacts resulting from large changes in NRM intensity (Roberts, 2006). These features might be attributable to dispersed ash particles that are coincident with at least several of the polarity events. One notable exception to this pattern occurs at 100 mcd (Fig. 4), which might represent an example of a short polarity interval associated with 'tiny wiggles' (e.g., Roberts and Lewin-Harris, 2000) that are observed in seafloor magnetic anomaly profiles within the late middle Eocene (Cande and Kent, 1992).

Regardless, the short-lived polarity intervals identified here are not considered in the overall polarity zonation.

4.2 Planktonic foraminiferal biostratigraphy

Planktonic foraminiferal assemblages at Sites 1051 and 1260 are typical of those found in (sub)tropical oceans in the late middle Eocene and are indicative of planktonic foraminiferal Zones E11 through E13. Microfossil preservation is good with planktonic foraminifera showing some evidence of recrystallization; specimens are 'frosty', not 'glassy' (Sexton et al., 2006b).

We have identified *Orbulinoides beckmanni* at both ODP sites (Table 2). *O. beckmanni* has some morphological variability within its range, with a shift to a more encompassing final chamber (increased test sphericity) and an increasing number of small supplementary sutural apertures at the base of the final chamber and between the earlier chambers (Plates I and II). This leads to highly distinctive forms toward the top of its stratigraphic range (Plate II). Of note, we find no stratigraphic significance in the presence or absence of areal apertures or 'bulla-like' structures.

The relative abundance of *O. beckmanni* within the total planktonic foraminiferal assemblage is shown in Figure 5a and b. Using our new magnetic stratigraphy for subtropical ODP Site 1051, we determine the LO of *O. beckmanni* to 40.5 Ma using the geomagnetic polarity time scale of Cande and Kent (1992, 1995; Fig. 5a), in the upper half of chron C18r (106.15 mcd). At equatorial Site 1260, the LO of *O. beckmanni* occurs toward the base of chron C18r (58.87 mcd) around a half million years earlier (41.0 Ma, Fig. 5b).

At both sites, for several hundred thousand years following its LO, *O. beckmanni* remains low in relative abundance (<2%, Fig. 5). At Site 1051, where a longer record is available, an abrupt increase (to ~4-6%) in the relative abundance of *O. beckmanni* occurs toward the base of chron C18n.2n at 40.1 Ma. Its relative abundance then remains on average at 3% for approximately 600 kyr, followed by a decrease and eventual extinction of *O. beckmanni* within chron C18n.1n at 61.90 mcd (at 39.5 Ma). We are unable to identify the HO of *O. beckmanni* at Site 1260 because the sedimentary succession is truncated by a hiatus at 36.1 mcd, which spans approximately five million years of geological time (middle-late Eocene) (Shipboard Scientific Party, 2004).

4.3 Stable isotope records

At both sites, benthic foraminiferal $\delta^{18}O$ records gradually shift by ~1‰ to lower values within chron C18r coincident with an overall shift to higher $\delta^{13}C$ values (Fig. 5c and d). The stable isotope record at Site 1260 is truncated by a hiatus at the top of chron C18r, but at Site 1051, benthic $\delta^{18}O$ values reach a short-lived (~40 kyr) minimum in the base of chron C18n.2n (at 40.05 Ma) coincident with an abrupt 1‰ decrease in $\delta^{13}C$ values (Fig. 5). Subsequently, both benthic $\delta^{18}O$ and $\delta^{13}C$ values at Site 1051 increase rapidly, followed by a more gradual shift to overall higher values. There is good agreement between the amplitude and timing of the $\delta^{18}O$ shift in the bulk (Bohaty et al., 2009) and benthic $\delta^{18}O$ records (this study) at Site 1051. At Site 1260, superimposed on the longer-term patterns of stable isotope change are a number of discrete negative $\delta^{13}C$ excursions (~1‰) with a duration of ~40 kyr each at 40.3, 40.4, 41.2 and 41.4 Ma (Fig. 5d). The two oldest of these four excursions, occur prior

276 to the onset of the MECO and are not associated with any obvious lithological
277 changes (Shipboard Scientific Party, 2004). In contrast, the younger $\delta^{13}C$ excursions
278 at 40.3 and 40.4 Ma, superimposed on the shift to more positive $\delta^{13}C$ values during
279 the MECO are coincident with thin (1-2 cm thick) clay horizons (cf. the C19r event
280 already documented at Site 1260, Edgar et al. 2007). None of these $\delta^{13}C$ excursions
281 are readily discernible in the lower-resolution benthic $\delta^{13}C$ record of Site 1051 (Fig.
282 5d).
283
284 5. **Discussion**
285 ***5.1 Correlation to the Geomagnetic Polarity Time Scale***
286 We integrate our new magnetic polarity pattern with published datasets (Shipboard
287 Scientific Party, 1998; Ogg and Bardot, 2001) between 0 and 150 mcd identifying
288 nine distinct magnetozones (R1-N4; Fig. 6). The resulting polarity patterns provides a
289 correlation with the GPTS between chrons C19r and C17r (Fig. 6). From 150 to 90
290 mcd our interpretation is in good agreement with published records (Shipboard
291 Scientific Party, 1998; Ogg and Bardot, 2001). However, above 90 mcd our
292 interpretation differs from that of the Shipboard Scientific Party (1998) and Ogg and
293 Bardot (2001) significantly, resulting in a two million year offset (Fig. 6). This
294 discrepancy arises from our differentiation of chron C18 into subchrons C18n.2n,
295 C18n.1r and C18n.1n, leading to the re-assignment of magnetozone N2 to chron
296 C18n.2n, and of subsequent chrons, e.g., magnetozone R3 = chron C18n.1r, N3 =
297 chron C18n.1n, R4 = chron C17r and N4 = chron C17n. Chron C18n was not
298 differentiated in the earlier polarity scheme because interpretation of the polarity
299 pattern based on calcareous nannofossil datums suggested that C18n was very
300 condensed at this site (Fig. 6, Shipboard Scientific Party, 1998; Ogg and Bardot,

2001). Resulting sedimentation rates for Site 1051 are relatively uniform (~4 cm/kyr) and are consistent with planktonic foraminiferal and radiolarian datums (Fig. 6). However, existing age calibrations for the respective HO and LO of calcareous nannofossil taxa *Dictyococcites bisectus* and *Chiasmolithus oamaruensis* are offset by almost one million years from the new age model (Fig. 6) and indicate the need for further calibration of biostratigraphic datums to the GPTS.

5.2 Revised calibrations for the lowest and highest occurrence of Orbulinoides beckmanni

At Site 1051, high sedimentation rates, good magnetostratigraphic control and high-resolution sampling allow us to directly calibrate the LO and HO of *Orbulinoides beckmanni* to the GPTS. Using our new age model for Site 1051, and the published refined magnetic stratigraphy from Site 1260 (Suganuma and Ogg, 2006; Edgar et al., 2007), a 500 kyr offset is evident in the position of the LO of *O. beckmanni* between Sites 1051 and 1260 (Fig. 5a and b). While the LO of *O. beckmanni* at Site 1051 in chron C18r (40.5 Ma) is consistent with that indicated by Berggren et al. (1995), at Site 1260 it is earlier (at the base of chron C18r at 41.0 Ma). The diachroneity reported here exceeds the uncertainties that are reasonably attributable to methodological (±<13 kyr) or age model inconsistencies (±<38 kyr) and is therefore interpreted to represent genuine geological diachrony between the two Atlantic Ocean sites of ~500 kyr. Consistent with the latitudinal diachrony observed between 2°S (Site 1260) and 25°N (Site 1051) is the later LO of *O. beckmanni* reported at 40.2±0.04 Ma (in the top part of chron C18r) at ~40°N in the Contessa Highway section, Italy (Jovane et al., 2007) (Fig 2). Recognition of the regionally diachronous LO of *O. beckmanni* has probably gone undetected previously because of the lack of

sections available on which the LO and HO can be tied directly to the GPTS.

Of note, the HO of *O. beckmanni* recorded here at Site 1051 in magnetochron C18n.1n is much later (600 kyr) than that reported in a recent calibration of its HO to 40.0 Ma in chron C18n.2n at ODP Site 1052 (Wade, 2004). This discrepancy is most likely attributable to the equivocal recognition and subdivision of chron C18n at Site 1052 (Ogg and Bardot, 2001), and is further complicated by the proposal of a 600 kyr-long hiatus (Pälike et al., 2001). Because the LO and HO of *O. beckmanii* defines the upper and lower boundaries of planktonic foraminiferal Zone E12, this zone at Site 1051 is at least 400 kyr longer than existing calibrations (Berggren and Pearson, 2005).

5.3 *Environmental controls on* Orbulinoides beckmanni's *biogeography*

We invoke an environmental control on the biogeography of *O. beckmanni* to explain the observed diachroneity in its lowest occurrence and its short total range duration. Expansion of species ranges from the tropics to higher latitudes is a common source of diachrony in first appearances of marine plankton (Kennett, 1970; Moore et al., 1993; Raffi et al., 1993; Spencer-Cervato et al., 1994; Kucera and Kennett, 2000; Sexton and Norris, 2008). Although little is known about the palaeoecology of *O. beckmanni*, this species is restricted to tropical and warm mid-latitudes (Bolli et al., 1972; Premoli Silva et al., 2006;) between ~30ºS and 45ºN, highlighted in our compilation of geographic occurrence (Fig. 2), suggesting that sea surface temperature (SST) may have played a major role in its geographic distribution. As surface waters warmed during the MECO (Bohaty and Zachos, 2003; Bohaty et al., 2009), conditions may have become more favorable for this taxon at higher latitudes

thereby allowing geographic range expansion to ~45°N (Fig. 2).

The HO of *O. beckmanni* post-dates the MECO at Site 1051 by at least 600 kyr (Fig. 5) which indicates that the apparent abrupt cooling at the termination of the MECO was not sufficient to completely eliminate this species from Site 1051. However, SST continued to decrease (Bohaty et al., 2009) and may have fallen below a critical threshold necessary to sustain viable population numbers. Despite the undoubted diagenetic overprint on the bulk sediment record, $\delta^{18}O$ values at the LO and HO of *O. beckmanni* are similar (~0.7‰, Fig. 5c), which is compatible with a thermal threshold controlling *O. beckmanni's* distribution. This also raises the possibility that the HO of *O. beckmanni* may be latitudinally diachronous. This interpretation is in keeping with the earlier HO of *O. beckmanni* (39.9 Ma, base of chron C18n.2n) at 40°N in the Contessa section (Jovane et al., 2007; Fig. 2). *O. beckmanni* is not confined to the MECO event and thus, by definition, this species cannot be termed an 'excursion taxon'. Nevertheless, the relatively short range of *O. beckmanni* (<1 Myr), combined with the coincidence of its peak abundance with peak ocean warmth, implies that this taxon had a narrow environmental tolerance and/or the ecological niche that it occupied disappeared because of cooling surface waters (Fig. 5c).

5.4 Constraints on the timing and environmental impact of the MECO

Our correlation of the magnetostratigraphic records to the GPTS suggests that the transient $\delta^{18}O$ and $\delta^{13}C$ shifts observed across the chron C18r/18n boundary at Sites 1260 and 1051 (Fig. 5c and d) are low latitude representations of the MECO. These are the first detailed records from the (sub)tropics and demonstrate that the MECO is a truly global event. The magnitude, relative timing and pattern of stable isotope

change are consistent with published benthic foraminiferal (e.g., ODP Site 748, Fig. 5c; Bohaty and Zachos, 2009) and bulk sediment (Jovane et al., 2007; Bohaty et al., 2009; Spofforth et al., 2010) stable isotope records from other ocean basins, which implies that the gradual onset and abrupt $\delta^{18}O$ maximum are reliable for global stratigraphic correlation (Fig. 5c and d).

At present it is unclear whether the higher-resolution features, notably, the two $\delta^{13}C$ excursions preceding the MECO peak at Site 1260, are also global in character. Because these excursions are coincident with clay layers which imply carbonate dissolution, they are reminiscent of simultaneous transient CCD shoaling and negative isotopic shifts associated with small inferred 'hyperthermal' events reported in other parts of the Eocene (e.g., Lourens et al., 2005; Edgar et al., 2007; Quillévéré et al., 2008). If these excursions prove to be present in other deep-sea sites, they may help to shed light on the mechanisms driving warming during the MECO.

6. Conclusions

We present new stable isotopic, magnetostratigraphic, and biostratigraphic records from (sub)tropical Atlantic ODP Sites 1051 and 1260 for the late middle Eocene, spanning the MECO. These represent the first detailed records of the MECO from the tropics and subtropics and demonstrate that the event is truly global. Closely associated with the MECO is the range and abundance variations of the biostratigraphically important planktonic foraminiferal species *O. beckmanni*. Detailed abundance counts of this species reveal a latitudinal diachrony of ~500 kyrs in its lowest occurrence, observed 500 kyrs earlier in the tropics (41.0 Ma at Site 1260) than in the subtropics (40.5 Ma at Site 1051). This latitudinal diachrony is

attributed to the poleward expansion of warm surface waters during the onset of the MECO, which created favorable conditions at extra-tropical latitudes for this thermophyllic species. Using our high-resolution magnetic polarity record at ODP Site 1051, the diachronous FO of *O. beckmanni* occurs within chron C18r and its disappearance within chron C18n.1n at 39.5 Ma, 600 kyr younger than previously reported. The disappearance of *O. beckmanni* from the subtropics is likely related to progressive cooling of sea surface waters below some critical threshold rather than to abrupt environmental change.

Acknowledgements

We thank M. Bolshaw, G. Paterson, R. Pearce and D. Spanner for help with laboratory work, and S. Bohaty for access to stable isotope data from ODP Sites 748 and 1051. Bridget Wade and an anonymous reviewer are thanked for their constructive reviews of this manuscript. Financial support was provided by a NERC small grant to SJG and PAW, a NERC CASE studentship (with Perkin Elmer) to KME and a NERC UKIODP Rapid Response Grant to PFS. This work used samples provided by the Ocean Drilling Program (ODP). The ODP (now IODP) is sponsored by the US National Science Foundation and participating countries under the management of the Joint Oceanographic Institutions (JOI), Inc.

References

Arthur, M.A. and Natland, J.H., 1979. Carbonaceous sediments in the North and South Atlantic: The role of salinity in stable stratification of Early Cretaceous basins.

In: Talwani, M.E.A. (Ed.), Deep Drilling Results in the Atlantic Ocean: Continental Margins and Palaeoenvironment. American Geophysical Union, Maurice Ewing Series 3, pp. 375-401.

Babic, L., Kuûenjak, M.H., Coric, S. and Zupanic, J., 2007. The middle Eocene age of the supposed late Oligocene sediments in the flysch of the Pazin Basin (Istria, Outer Dinarides). Croatian Natural History Museum 16, 83-103.

Berggren, W.A., Kent, D.V., Swisher, C. and Aubry, M.-P., 1995. A revised Cenozoic geochronology and chronostratigraphy. In: Berggren, W.A., Kent, D.V., Aubrey, M.-P. and Hardenbol, J. (Eds.), Geochronology, Time-Scales and Global Stratigraphic Correlation. Tulsa, SEPM Special Publiciation 54, pp. 129-212.

Berggren, W.A. and Pearson, P.A., 2005. A revised tropical to subtropical planktonic foraminiferal zonation of the Eocene and Oligocene. Journal of Foraminiferal Research 35, 279-298.

Bohaty, S.M. and Zachos, J.C., 2003. Significant Southern Ocean warming in the late middle Eocene. Geology 31, 1017-1020.

Bohaty, S.M., Zachos, J.C., Florindo, F. and Delaney, M.L., 2009. Coupled greenhouse warming and deep-sea acidification in the middle Eocene. Paleoceanography 24, PA2207 doi:10.1029/2008PA001676.

Bolli, H.M., 1972. The genus *Globigerinatheka* Brönnimann. Journal of Foraminiferal

Research 2, 109-136.

BouDagher-Fadel, M. and Clark, G.N., 2006. Stratigraphy, palaeoenvironment and palaeogeography of Maritime Lebanon: a key to Eastern Mediterranean Cenozoic history. Stratigraphy 3, 81-118.

Bralower, T.J., Premoli Silva, I., Malone, M.J., et al., 2002. Proceedings of the Ocean Drilling Program Initial Reports 198. College Station, Texas (Ocean Drilling Program).

Cande, S.C. and Kent, D.V., 1992. A new geomagnetic polarity time scale for the Late Cretaceous and Cenozoic. Journal of Geophysical Research 97, 13917-13951.

Cande, S.C. and Kent, D.V., 1995. Revised calibration of the geomagnetic polarity timescale for the Late Cretaceous and Cenozoic. Journal of Geophysical Research 100, 6093-6095.

Curry, W.B. Shackleton, N.J., Richter, C., et al., 1995. Proceedings of the Ocean Drilling Program Initial Reports, 154. College Station, Texas (Ocean Drilling Program).

Edgar, K.M., Wilson, P.A., Sexton, P.F. and Suganuma, Y., 2007. No extreme bipolar glaciation during main Eocene compensation shift. Nature 448, 908-911.

Gradstein, F.M., Ogg, J.G. and Smith, A.G., 2004, A Geologic Time Scale 2004.

476 Cambridge University Press.

477

478 Jovane, L., Florindo, F., Coccioni, R., Dinarès-Turell, J., Marsili, A., Monechi, S.,
479 Roberts, A.P. and Sprovieri, M., 2007. The middle Eocene climatic optimum event in
480 the Contessa Highway section, Umbrian Apennines, Italy. Geological Society of
481 America Bulletin 119, 413-427.

482

483 Karig D.E., Ingle, J.C.Jr., et al., 1975. Initial Reports of the Deep Sea Drilling Project
484 31, Washington (U.S. Government Printing Office).

485

486 Katz, M.E., Katz, D.R., Wright, J.D., Miller, K.G., Pak, D.K., Shackleton, N.J. and
487 Thomas, E., 2003. Early Cenozoic benthic foraminiferal isotopes: species reliability
488 and interspecies correction factors. Paleoceanography 18, 1024, doi:
489 10.1029/2002PA000798.

490

491 Kelly, D.C., Bralower, T.J., Zachos, J.C., Premoli-Silva, I. and Thomas, E., 1996.
492 Rapid diversification of planktonic foraminifera in the tropical Pacific (ODP Site 865)
493 during the latest Paleocene thermal maximum. Geology 24, 423-426.

494

495 Kelly, D.C., Bralower, T.J., Zachos, J.C., 1998. Evolutionary consequences of the
496 latest Paleocene thermal maximum for tropical planktonic foraminifera.
497 Palaeogeography, Palaeoclimatology, Palaeoecology 141, 139-161.

498

499 Kennett, J.P., 1970, Pleistocene palaeoclimates and foraminiferal biostratigraphy in
500 subantarctic deep-sea cores: Deep-Sea Research, A, 17, 125–140.

Kirschvink, J.L., 1980. The least-squares line and plane and line analysis of palaeomagnetic data. Geophysical Journal of the Royal Astronomical Society 62, 699-718.

Kucera, M. and Kennett, J.P., 2000. Biochronology and evolutionary implications of Late Neogene California margin planktonic foraminiferal events. Marine Micropalaeontology 40, 67-81.

Lowrie, W., Alvarez, W., Napoleone, G., Perch-Nielson, K., Premoli Silva, I. and Tomarkine, M., 1982. Palaeogene magnetic stratigraphy in Umbrian pelagic carbonate rocks: the Contessa sections, Gubbio. Geological Society of America Bulletin 93, 414-432.

Luciani, V., Giusberti, L., Agnini, C., Fornaciari, E., Rio, D., Spofforth, D.J., Pälike, 2010. Ecological and evolutionary response of tethyan planktonic foraminifera to the middle Eocene climatic optimum (Meco) from the Alano section (NE Italy). Palaeogeography, Palaeoclimatology, Palaeoecology 292, 82-95.

Lyle, M., Wilson, P.A., Janecek, T.R. et al., 2002. Proceedings of the Ocean Drilling Program Initial Reports 199. College Station, Texas (Ocean Drilling Program).

Lyle, M., Olivarez-Lyle, A., Backman, J. and Tripati, A., 2005. Biogenic sedimentation in the Eocene equatorial Pacific – the stuttering greenhouse and Eocene compensation depth. In: Wilson, P.A., Lyle, M. and Firth, J.V. (Eds.), Proceedings of

526 the Ocean Drilling Program Scientific Results 199. College Station, Texas (Ocean
527 Drilling Program), doi:10.2973/odp.proc.sr.199.219.2005.
528
529 Moore, T.C., Shackleton, N.J. and Pisias, N.G., 1993. Paleoceanography and the
530 diachrony of radiolarian events in the eastern equatorial Pacific. Paleoceanography 8,
531 567-586.
532
533 Napoleone, G., Premoli Silva, I., Heller, F., Cheli, P., Corezzi, S. and Fischer, A.F.,
534 1983. Eocene magnetic stratigraphy at Gubbio, Italy, and its implications for
535 Palaeogene geochronology. Geological Society of America Bulletin 94, 181-191.
536
537 Norris, R.D., Kroon, D., Klaus, A. et al., 1998. Proceedings of the Ocean Drilling
538 Program Initial Reports 171B. College Station, Texas (Ocean Drilling Program).
539
540 Ogg, J.G. and Bardot, L., 2001. Aptian through Eocene magnetostratigraphic
541 correlation of the Blake Nose Transect (Leg 171B), Florida continental margin. In:
542 Kroon, D., Norris, R.D., and Klaus, A. (Eds.), Proceedings of the Ocean Drilling
543 Program Scientific Results 171B: College Station, Texas (Ocean Drilling Program),
544 doi:10.2973/odp.proc.sr.171b.104.2001.
545
546 Pälike, H., Shackleton, N.J. and Röhl, U., 2001, Astronomical forcing in late Eocene
547 marine sediments. Earth and Planetary Science Letters 193, 589-602.
548
549 Premoli Silva, I., Wade, B.S. and Pearson, P.N., 2006, Taxonomy of Globigerinatheka
550 and Orbulinoides. In: Pearson, P.N., Olsson, R.K., Huber, B.T., Hemleben, C. and

551 Berggren, W.A. (Eds.), Atlas of Eocene Planktonic Foraminifera. Cushman
552 Foundation Special Publication, 41, pp. 169-212.
553
554 Proto Decima, F. and Bolli, H., 1970. Evolution and variability of *Orbulinoides*
555 *beckmanni* (Saito). Eclogae Geologicae Helvetiae. 63, 883-905.
556
557 Raffi, I., Backman, J., Rio, D. and Shackleton, N.J., 1993. Plio-Pleistocene
558 nannofossil biostratigraphy and calibration to oxygen isotope stratigraphies from
559 Deep Sea Drilling Project Site 607 and Ocean Drilling Program Site 677.
560 Paleoceanography 8, 387-403.
561
562 Roberts, A.P., 2006. High-resolution magnetic analysis of sediment cores: strengths,
563 limitations and strategies for maximizing the value of long-core magnetic data.
564 Physics of the Earth and Planetary Interiors, 156, 162-178.
565
566 Roberts, A.P. and Lewin-Harris, J.C., 2000, Magnetic marine anomalies: evidence
567 that 'tiny wiggles' represent short-period geomagnetic polarity intervals, Earth and
568 Planetary Science Letters, 183, 375-388.
569
570 Sager, W.W., Winterer, E.L., Firth, J.V., et al., 1993, Proceedings of the Ocean
571 Drilling Program Initial Reports 143. College Station, Texas (Ocean Drilling
572 Program).
573
574 Schrag, D.P., Depaolo, D.J. and Richter, F.M., 1995, Reconstructing past sea-surface
575 temperatures - correcting for diagenesis of bulk marine carbonate, Geochimica et

576 Cosmochimica Acta, 59, 2265-2278.

577

578 Sexton, P.F., Wilson, P.A. and Norris, R.D., 2006a, Testing the Cenozoic multisite
579 composite $\delta^{18}O$ and $\delta^{13}C$ curves: new monospecific Eocene records from a single
580 locality, Demerara Rise (Ocean Drilling Program Leg 207), Paleoceanography, 21,
581 PA2019, doi:10.1029/2005PA001253.

582

583 Sexton, P.F., Wilson, P.A. and Pearson, P.N., 2006b, Microstructural and
584 geochemical perspectives on planktic foraminiferal preservation: "glassy" versus
585 "frosty". Geochemistry, Geophysics, Geosystems 7, Q12P19,
586 doi:10.1029/2006GC001291.

587

588 Sexton, P.F., and Norris, R.D. 2008, Dispersal and biogeography of marine plankton:
589 long-distance dispersal of the foraminifer *Truncorotalia truncatulinoides*, Geology,
590 36, 899-902.

591

592 Shipboard Scientific Party, 1998. Site 1051. In: Norris, R.D., Kroon, D., Klaus, A. et
593 al., (Eds.), Proceedings of the Ocean Drilling Program Initial Reports 171B. College
594 Station, Texas (Ocean Drilling Program).

595

596 Shipboard Scientific Party, 2004. Site 1260. In: Erbacher, J., Mosher, D.C., Malone,
597 M.J. et al. (Eds.), Proceedings of the Ocean Drilling Program Initial Reports 207.
598 College Station, Texas (Ocean Drilling Program).

599

600 Spencer-Cervato, C., Thiersten, H.R., Lazarus, D.B. and Beckmann, J-P., 1994. How

601 synchronous are Neogene marine plankton events? Paleoceanography 9, 739-763.
602
603 Suganuma, Y. and Ogg, J.G., 2006. Campanian through Eocene magnetostratigraphy
604 of Sites 1257-1261, ODP Leg 207, Demerara Rise (western equatorial Atlantic). In:
605 Mosher, D.C., Erbacher, J. and Malone, M.J. (Eds.), Proceedings of the Ocean
606 Drilling Program Scientific Results 207: College Station, Texas (Ocean Drilling
607 Program).
608
609 Tjalsma, R.C. and Lohmann, G.P., 1983. Paleocene-Eocene bathyal and abyssal
610 benthic foraminifera from the Atlantic Ocean. Micropalaeontology Special
611 Publication 4.
612
613 van Morkhoven, F.P.C.M., Berggren, W.A. and Edwards, A.S., 1986. Cenozoic
614 cosmopolitan deep-water benthic foraminifera. Elf-aquitaine, Pau.
615
616 Wade, B.S., 2004. Planktonic foraminiferal biostratigraphy and mechanisms in the
617 extinction of *Morozovella* in the late middle Eocene. Marine Micropalaeontology 51,
618 23-38.
619
620 Zachos, J.C., Kroon, D., Blum, P., et al., 2004. Proceedings of the Ocean Drilling
621 Program Initial Reports 208. College Station, Texas (Ocean Drilling Program).
622
623 Zachos, J.C., Dickens, G.R. and Zeebe, R.E., 2008. An early greenhouse perspective
624 on greenhouse warming and carbon-cycle dynamics. Nature 451,
625 doi:10.1038/nature06588.

626

627 ***Figure captions***

628

629 Figure 1 – Study interval in the context of Cenozoic climate trends. a) Cenozoic
630 benthic foraminiferal $\delta^{18}O$ record modified from Zachos et al. (2008). The MECO is
631 shown on a revised age scale in keeping with this study. b) The Geomagnetic polarity
632 time scale used follows Cande and Kent (1992; 1995). New 'E' planktonic
633 foraminiferal tropical biozonation scheme from Berggren and Pearson (2005), and 'P'
634 tropical biozonation scheme from Berggren et al. (1995). c) Benthic foraminiferal
635 $\delta^{18}O$ record from Site 748, Southern Ocean (Bohaty et al., 2009). Black vertical line
636 represents the duration of the MECO based on the $\delta^{18}O$ stable isotope pattern. Black
637 dashed lines denote the position of the MECO relative to the GPTS and tropical
638 zonation scheme. Grey boxes denote the study interval and the black vertical line
639 represents the duration of the MECO based on the $\delta^{18}O$ pattern.

640

641 Figure 2 – Palaeogeographic reconstruction of the Eocene illustrating the presence
642 and absence of *Orbulinoides beckmanni*. ODP Sites 1051 and 1260 (stars) used in this
643 study. Solid circles indicate the presence and open circles the absence of *O.*
644 *beckmanni*. Data are compiled from deep-sea drill sites and exposed marine sections
645 that coincide with planktonic foraminiferal Zone E12 but are not necessarily
646 stratigraphically 'complete' sections. Data are compiled from Lowrie et al. (1982),
647 BouDagher-Fadel and Clark (2006), Pearson et al. (2006), Babic et al. (2007), Jovane
648 et al. (2007) and http://www-odp.tamu.edu/database/. To prevent bias, sites where *O.*
649 *beckmanni* is absent because of hiatuses, dissolution, lack of carbonate or non-
650 recovery of this stratigraphic interval are excluded. The base map for 40 Ma was

651 generated from www.odsn.de/odsn/series/palaeomap/palaeomap.html.

652

653 Figure 3 – Typical AF (alternating field) demagnetization behavior of sediments from
654 ODP Site 1051. a-f) samples with stable demagnetization behaviour. g-h) samples
655 with less-stable demagnetization behaviour. In the vector component diagrams, open
656 symbols represent projections onto the vertical plane and closed onto the horizontal
657 plane. Jmax is the NRM value measured during AF demagnetization.

658

659 Figure 4 – Down-core variations in the intensity of the natural remanent
660 magnetization (NRM) and inclination for ODP Site 1051. a) Inclination data from
661 Ogg and Bardot (2001). Closed symbols represent data points with maximum angular
662 deviation (MAD) values of <10º, while open data points have MAD values between
663 10º and 15º. b) MAD values of data shown in panels c and d. c) NRM intensity after
664 AF demagnetization at 25 mT for samples shown in panel c. d) Inclination data for the
665 shipboard composite depth sections (mcd – meters composite depth). Grey symbols =
666 data from Hole A and black symbols from Hole B, with MAD values of <10º (this
667 study). Horizontal dashed lines represent splice points. The magnetic polarity
668 zonation is shown on the right. Black represents normal and white represents reversed
669 polarity intervals.

670

671 Figure 5 – Stable isotope records across the middle Eocene climatic optimum and
672 relative abundance records of *O. beckmanni*. Relative abundance records of *O.*
673 *beckmanni* at ODP Sites 1051 (panel a) and 1260 (panel b). Horizontal black lines
674 denote core depths between which the lowest and highest occurrences (LO and HO)
675 of *O. beckmanni* were recorded by the Shipboard Scientific Parties (1998; 2004).

676 Revised planktonic foraminiferal zone boundaries based on this study shown. Arrows
677 indicate new placement of the boundaries of Zone E12. c) Benthic foraminiferal $\delta^{18}O$
678 records from Sites 1051 and 1260 (this study). Starred (*) records are from Bohaty et
679 al. (2009) and are aligned on the new Site 1051 age model. d) Benthic foraminiferal
680 $\delta^{13}C$ records from Sites 1051 and 1260 (this study). Starred (*) records are from
681 Bohaty et al. (2009) and are aligned on the new Site 1051 age model.
682
683 Figure 6 - Age versus depth plot with correlation of the ODP Site 1051 polarity
684 zonation to the geomagnetic polarity time scale of Cande and Kent (1992, 1995).
685 Calcareous plankton and radiolarian datums determined by the Shipboard Scientific
686 Party (1998) are shown by colored diamonds (errors indicated by vertical black lines).
687 Ages are from Berggren et al. (1995), with the exception of the highest occurrence
688 (HO) of *O. beckmanni* and the extinction of *Morozovelloides* and large acarininids,
689 which are from Wade (2004). Revised placement of the LO and HO of *O. beckmanni*
690 are shown by solid circles. Polarity intervals marked 'R' have reversed polarity and
691 those marked 'N' have normal polarity. mcd = metres composite depth. The grey line
692 represents the age model from SSP'98 = Shipboard Scientific Party (1998) and
693 O&B'01 = Ogg and Bardot (2001).
694
695 Plate I - Scanning electron microscope images from ODP Site 1051 that illustrate
696 morphological development within the clade leading to *Orbulinoides beckmanni*.
697 Scale bars are 100 µm. (a) *Subbotina senni*, Sample 1051B 7H-5, 65-66 cm. (b)
698 *Globigerinatheka subconglobata*, Sample 1051B 9H-5, 35-37 cm. (c)
699 *Globigerinatheka barri*, Sample 1051B 9H-5, 35-37 cm. (d) *Globigerinatheka*
700 *kugleri*, Sample 1051B 11H-2, 65-67 cm. (e) *Globigerinatheka curryi*, Sample 1051B

11H-3, 131-133 cm. (f) *Globigerinatheka mexicana*, Sample 1051B-11H-4, 65-67 cm. (g) *Globigerinatheka euganea*, Sample 1260A 6R-1, 7-8.5 cm. (h) *Globigerinatheka euganea*, Sample 1051B 11H-3, 145-147 cm. (i) *Orbulinoides beckmanni*, Sample 1051B 11H-3, 131-133 cm. (j) .*Orbulinoides beckmanni*, Sample 1051B 9H-5, 35-37 cm. (k) *Orbulinoides beckmanni*, Sample 1051B 11H-3, 131-133 cm. (l) *Orbulinoides beckmanni*, Sample 1051B 9H-5, 5-7 cm.

Plate II - Scanning electron microscope images from ODP Sites 1051 and 1260 that illustrate morphological variability within *Orbulinoides beckmanni*. Scale bars are 100 μm. (a) *Orbulinoides beckmanni*, Sample 1051B 8H-2, 105-107 cm. (b) *Orbulinoides beckmanni*, Sample 1051B 8H-2, 105-107 cm. (c) *Orbulinoides beckmanni*, Sample 1051B 8H-2, 105-107 cm. (d) *Orbulinoides beckmanni*, Sample 1051A 8H-4, 45-47 cm. (e) *Orbulinoides beckmanni*, Sample 1051A 8H-4, 45-47 cm. (f) *Orbulinoides beckmanni*, Sample 1051A 8H-4, 45-47 cm. (g) *Orbulinoides beckmanni*, Sample 1051A 8H-6, 5-7 cm. (h) *Orbulinoides beckmanni*, Sample 1051A 8H-6, 5-7 cm. (i) *Orbulinoides beckmanni*, Sample 1051A 8H-6, 5-7 cm. (j) *Orbulinoides beckmanni*, Sample 1260A 6R-1, 7-8.5 cm. (k) *Orbulinoides beckmanni*, 1260A 6R-1, 7-8.5 cm. (l) *Orbulinoides beckmanni*, Sample 1260A 6R-1, 7-8.5 cm.

Table 1 – Polarity zones and interpretation of chrons for ODP Site 1051.

Table 2 – Comparison of magnetobiochronology of planktonic foraminiferal datum events identified by Berggren et al. (1995), *Wade (2004), and this study.

726
727

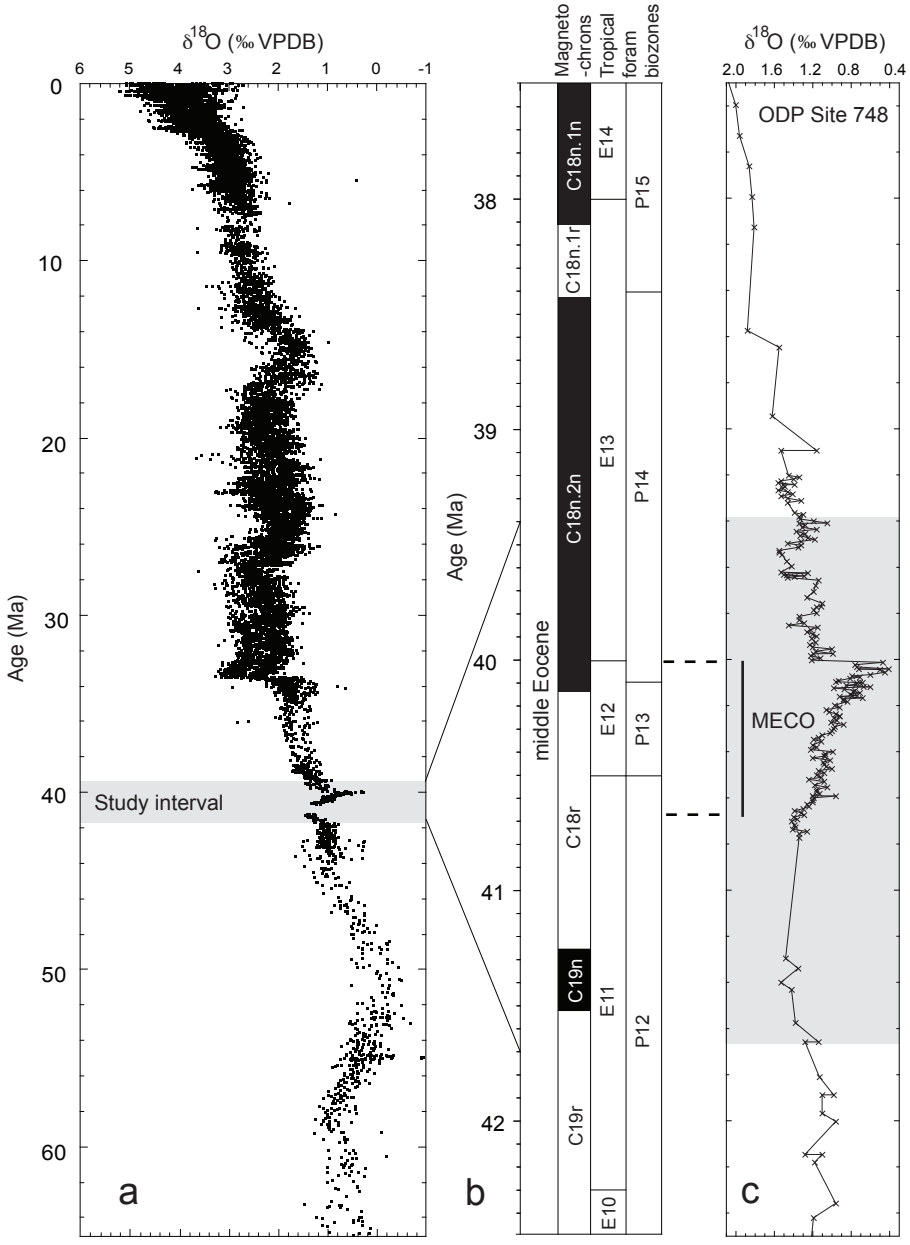

Edgar_Figure 1

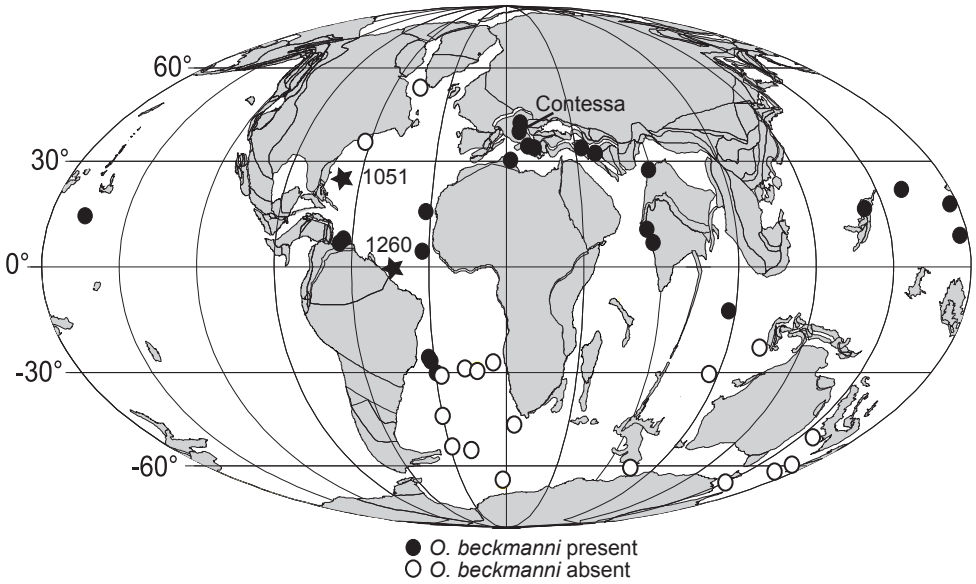

Edgar_Figure 2

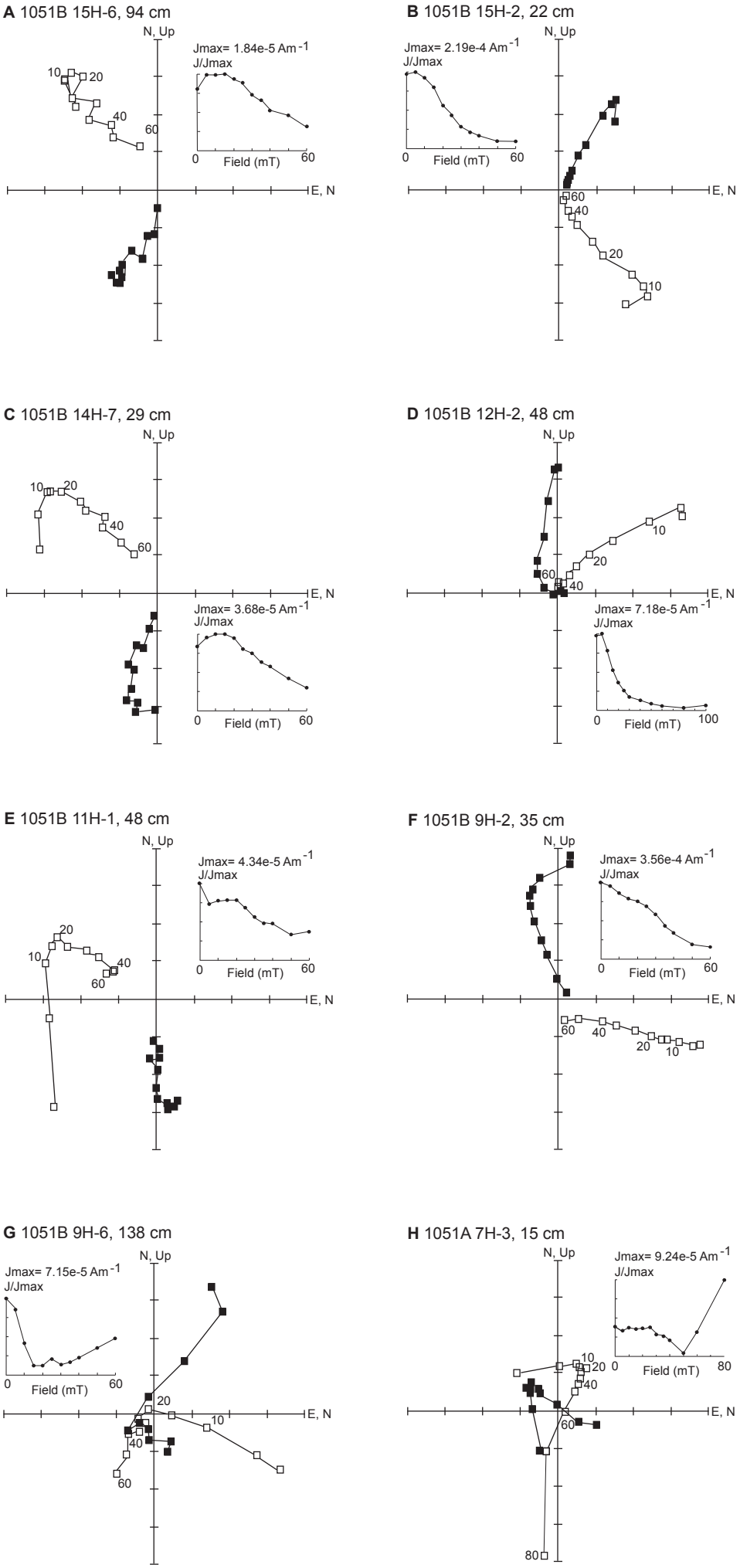

Edgar_Figure 3

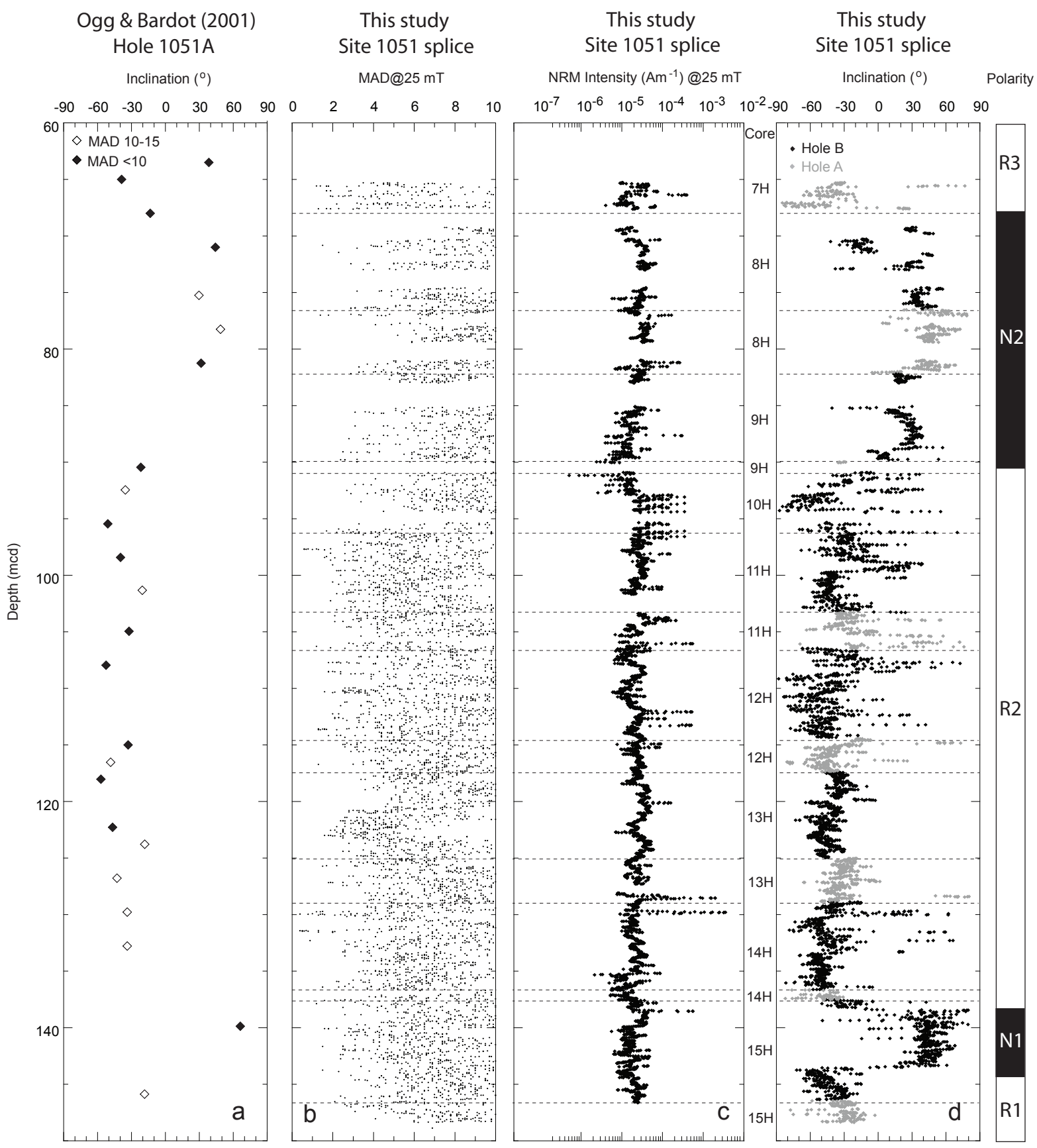

Edgar_Figure 4

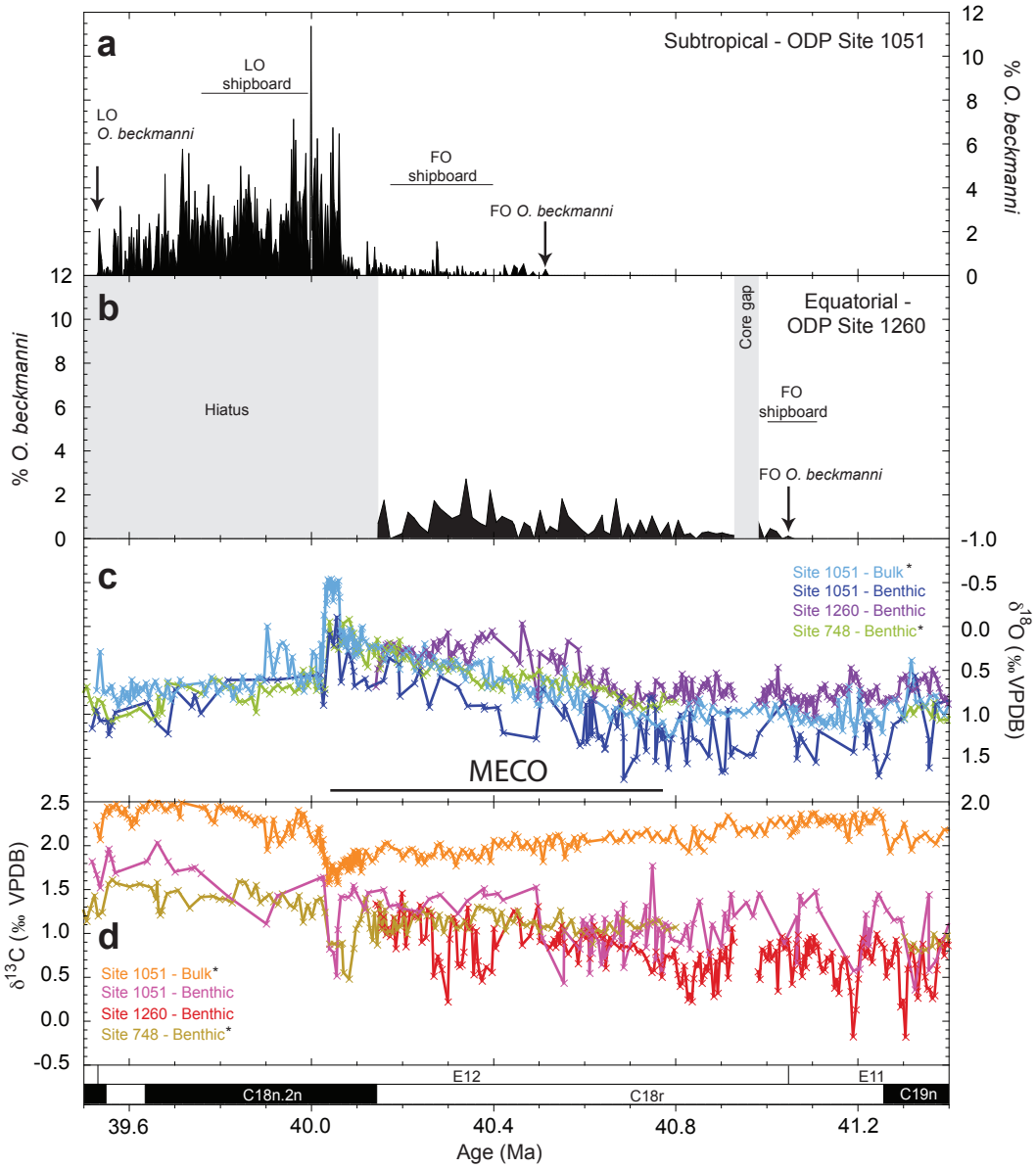

Edgar_Figure 5

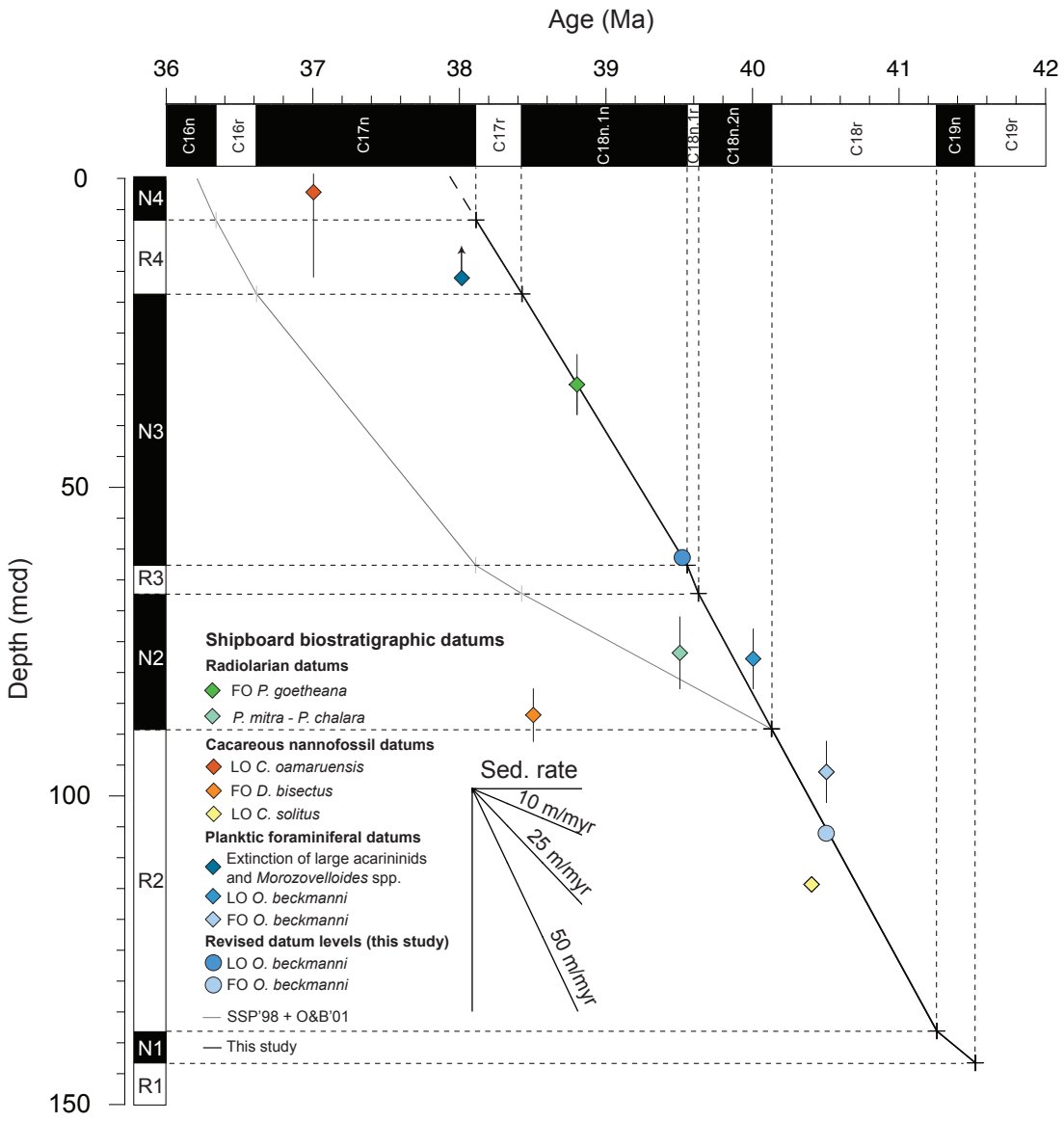
Age (Ma)
36
37
38
39
40
41
42
C16n
C16r
C17n
C17r
C18n.1n
C18n.1r
C18n.2n
C18r
C19n
C19r
Depth (mcd)
0
50
100
150
N4
R4
N3
R3
N2
R2
N1
R1
Shipboard biostratigraphic datums
Radiolarian datums
FO P. goetheana
P. mitra - P. chalara
Cacareous nannofossil datums
LO C. oamaruensis
FO D. bisectus
LO C. solitus
Planktic foraminiferal datums
Extinction of large acarininids and Morozovelloides spp.
LO O. beckmanni
FO O. beckmanni
Revised datum levels (this study)
LO O. beckmanni
FO O. beckmanni
SSP'98 + O&B'01
This study
Sed. rate
10 m/myr
25 m/myr
50 m/myr

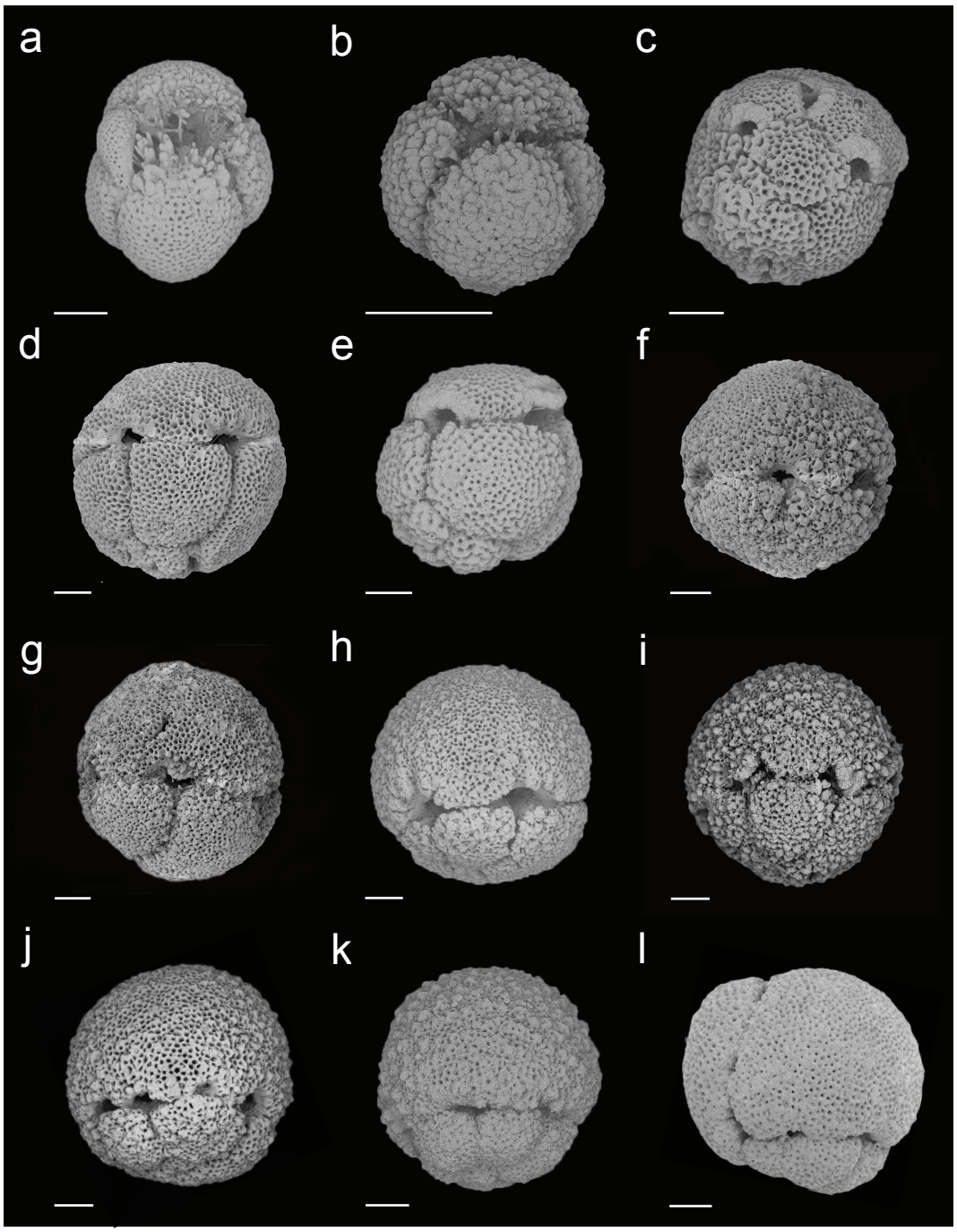

Edgar_Platel

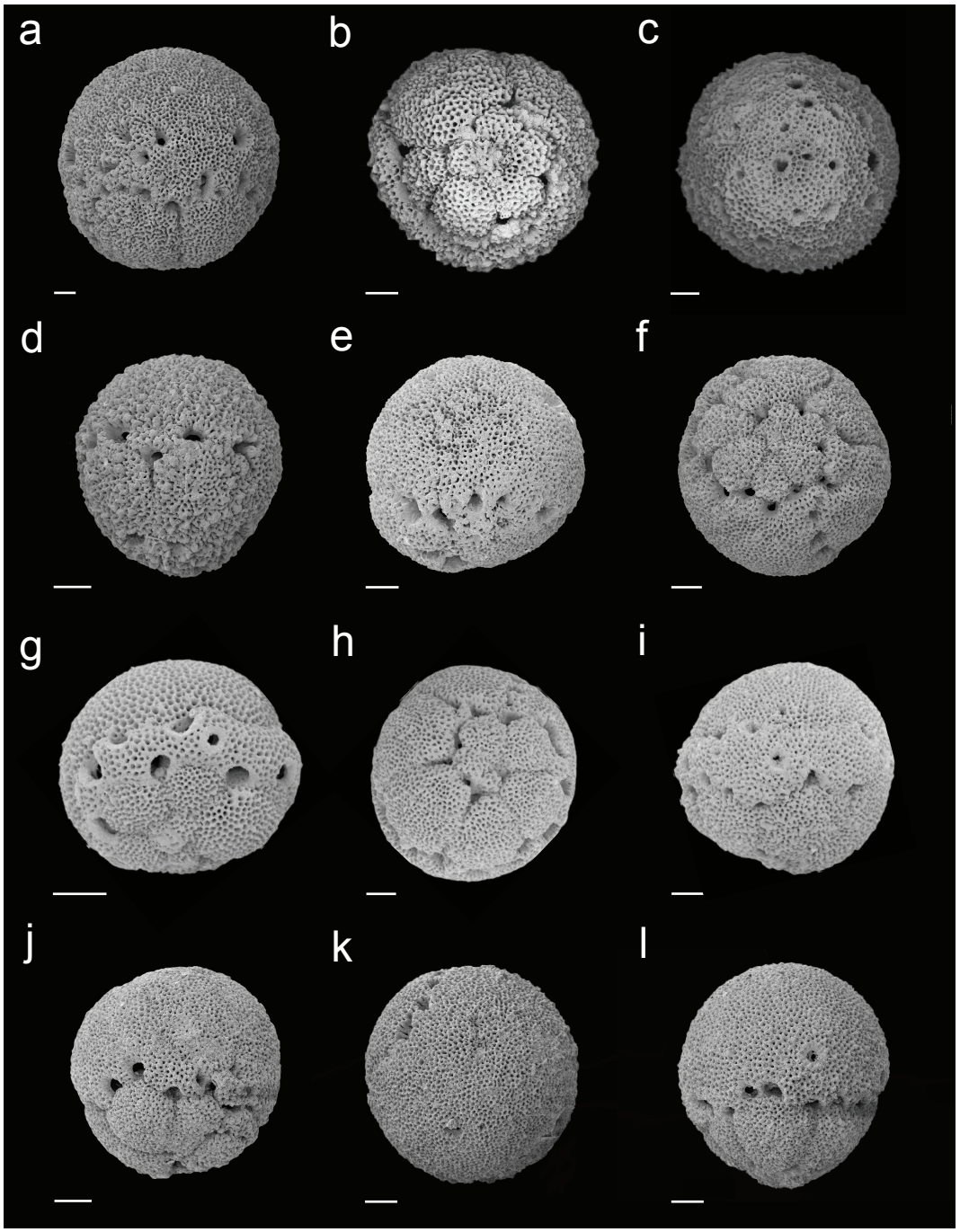

Edgar_Plate II

Table 1

Polarity zone	Chron (base)	OB&'01 T (mcd)	OB&'01 B (mcd)	This study T (mcd)	This study B (mcd)	Age CK95 (Ma)
-	C16n	7.00*	-	-	-	36.410
-	C16r	19.00*	-	-	-	36.618
N4	C17n	60.35	65.00	7.00*	-	38.113
R4	C17r	68.00	71.00	19.00*	-	38.426
N3	C18n.1n	-	-	60.35	65.00	39.552
R3	C18n.1r	-	-	67.52	67.54	39.631
N2	C18n.2n	-	-	88.90	90.00	40.130
R2	C18r	135.78	139.88	138.41	138.43	41.257
N1	C19n	142.88	145.88	143.52	143.54	41.521

Magnetochron ages from Cande and Kent (1992, 1995) referred to as CK95. N = normal, R = reverse, T = top, B= base and mcd = meters composite depth. * = magnetochron boundaries from the Shipboard Scientific Party (1998). OB&'01data from Ogg and Bardot (2001).

Datum	Shipboard study		Age CK95	Age GPTS04	This study		New Age CK95	Age GPTS04
	T (mcd)	B (mcd)	(Ma)	(Ma)	T (mcd)	B (mcd)	(Ma)	(Ma)
ODP Site 1051								
HO *O. beckmanni*	73.26	82.95	40.0*	39.4	61.80	61.90	39.5	39.0
LO *O. beckmanni*	91.45	101.35	40.5	39.8	106.15	106.45	40.5	39.8
ODP Site 1260								
LO *O. beckmanni*	57.80	59.30	40.5	39.8	58.87	59.17	41.0	40.4

Geomagnetic polarity time scales of Cande and Kent (1992, 1995) = CK95 and Gradstein et al., 2004 = GPTS04. LO and HO are lowest and highest occurrences, T = top and B = base, mcd = metres composite depth and * = Wade (2004).